# UniFlow: Towards Zero-Shot LiDAR Scene Flow for Autonomous Vehicles via Cross-Domain Generalization

Siyi Li<sup>1</sup>, Qingwen Zhang<sup>2</sup>, Ishan Khatri<sup>3</sup>, Kyle Vedder<sup>1</sup>, Deva Ramanan<sup>3</sup>, Neehar Peri<sup>3</sup> University of Pennsylvania<sup>1</sup>, KTH Royal Institute of Technology<sup>2</sup>, Carnegie Mellon University<sup>3</sup>

#### **Abstract**

LiDAR scene flow is the task of estimating per-point 3D motion between consecutive point clouds. Recent methods achieve centimeter-level accuracy on popular autonomous vehicle (AV) datasets, but are typically only trained and evaluated on a single sensor. In this paper, we aim to learn general motion priors that transfer to diverse and unseen LiDAR sensors. However, prior work in LiDAR semantic segmentation and 3D object detection demonstrate that naively training on multiple datasets yields worse performance than single dataset models. Interestingly, we find that this conventional wisdom does not hold for motion estimation, and that state-of-the-art scene flow methods greatly benefit from cross-dataset training. We posit that low-level tasks such as motion estimation may be less sensitive to sensor configuration; indeed, our analysis shows that models trained on fast-moving objects (e.g., from highway datasets) perform well on fast-moving objects, even across different datasets. Informed by our analysis, we propose UniFlow, a family of feedforward models that unifies and trains on multiple large-scale LiDAR scene flow datasets with diverse sensor placements and point cloud densities. Our frustratingly simple solution establishes a new state-of-the-art on Waymo and nuScenes, improving over prior work by 5.1% and 35.2% respectively. Moreover, UniFlow achieves stateof-the-art accuracy on unseen datasets like TruckScenes, outperforming prior TruckScenes-specific models by 30.1%. We include additional visuals on our project page.

#### 1. Introduction

Recent LiDAR scene flow methods achieve remarkable performance on popular autonomous vehicle (AV) datasets [12, 35, 36, 49] like Argoverse 2, nuScenes, and Waymo [1, 33, 44]. Notably, current state-of-the-art approaches train and evaluate on each dataset independently and do not attempt to generalize to unseen sensor configurations. Intuitively, since each dataset has different sensor placements and point cloud densities, training separate models for each domain *seems* reasonable (Figure 1). For example, Argov-

erse 2 (AV2) [44] uses two out-of-phase 32 beam LiDARs, nuScenes [1] uses one 32 beam sensor, and Waymo [33] uses a custom 64 beam sensor. Indeed, it is notoriously challenging to train multi-dataset models for LiDAR-based 3D object detection [31, 41] and semantic segmentation [14, 30] that improve over single dataset models. Interestingly, our analysis challenges this conventional wisdom for LiDAR-based scene flow. Unlike "high-level" tasks like LiDAR semantic segmentation or 3D object detection that require human-defined taxonomies [16], we argue that LiDAR scene flow models capture universal "low-level" geometric features that should, in principle, generalize better across sensors.

Cross-Domain Generalization for Low-Level Vision. Notably, we observe similar trends in RGB-based low-level vision tasks, where models learn generalizable geometric representations that transfer well across datasets. For example, FlowNet [5, 10] and RAFT [34] show that optical flow models trained on synthetic datasets (e.g. FlyingChairs, FlyingThings3D, Sintel) generalize surprisingly well to casually captured videos. More recently, zero-shot monocular depth estimators like MoGe [40] and monocular scene flow estimators like ZeroMSF [20] demonstrate that training on diverse datasets significantly improves zero-shot performance. Therefore, we posit that low-level LiDAR-based scene flow may similarly generalize to different sensors if trained at scale.

To better understand the problem, we first train dataset-specific models for AV2 [44], Waymo [33] and nuScenes [1] and evaluate zero-shot cross-domain performance. Surprisingly, Flow4D [15] trained on Waymo achieves similar Dynamic Mean EPE on AV2 as Flow4D trained on AV2. Importantly, Waymo's 64 beam LiDAR has considerably more point density than AV2's two out-of-phase 32-beam LiDARs (Fig. 1), indicating that point density does not significantly impact LiDAR scene flow generalization. Further, Flow4D (Waymo) achieves lower EPE (i.e. better performance) than Flow4D (AV2) on fast moving objects in AV2 since there are more fast movers in Waymo than in AV2 (Table 1). This suggests that the accuracy of motion prediction is highly correlated with object velocity (Figure

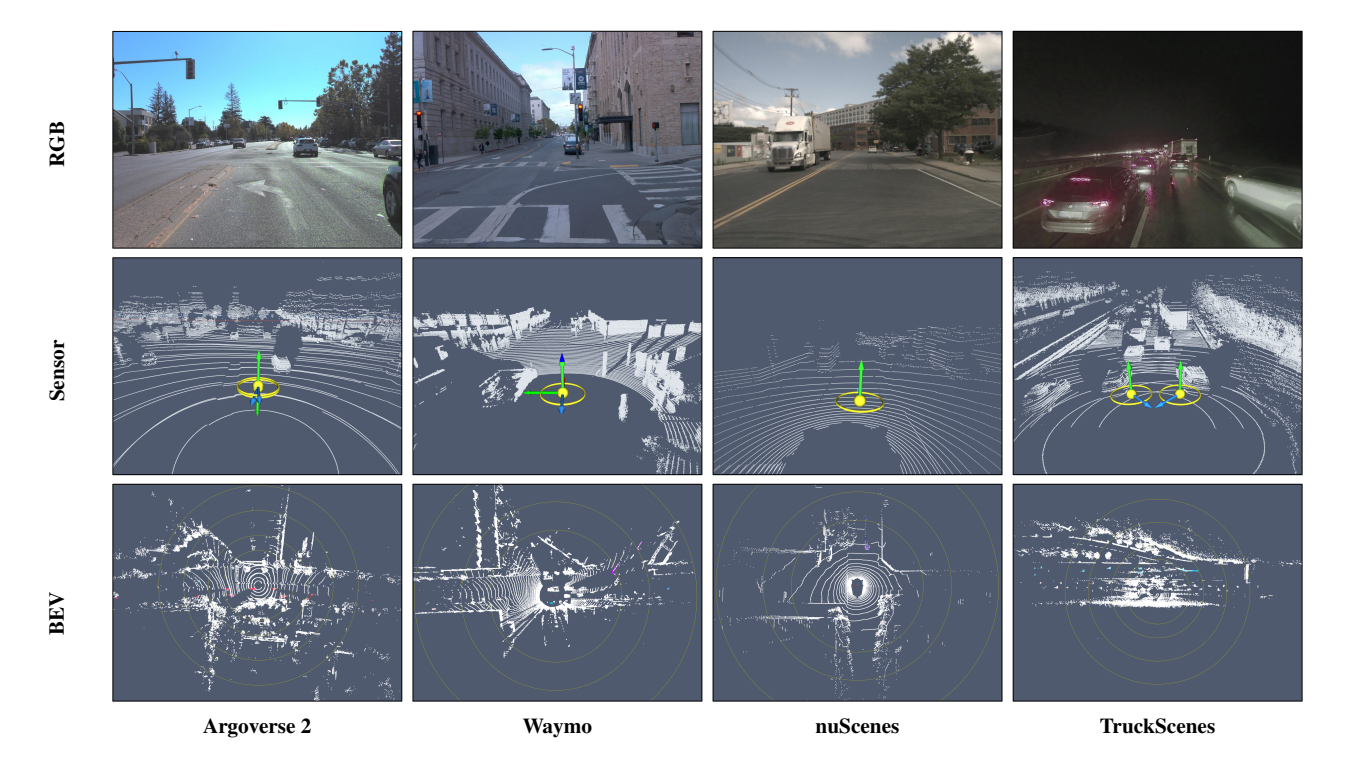


Figure 1. **Dataset Diversity.** We visualize the front-center RGB (top), LiDAR sensor positions (middle) and BEV LiDAR point clouds (bottom) for Argoverse 2, Waymo, nuScenes and TruckScenes. Notably, all four datasets use different sensors, and collect data in different environments. Specifically, Argoverse 2, Waymo, and nuScenes collect data in urban city centers with sedans, while TruckScenes primarily collects data on highways with a truck. Due to the diversity of environments and sensor configurations, contemporary LiDAR scene flow methods typically only train and evaluate on each dataset independently. However, we find that multi-dataset training significantly improves both in-domain and out-of-domain generalization. Note that RGB images are shown for visualization purposes only; we address LiDAR-only scene flow for AVs.

2); in order to accurately predict fast motion, one should train on fast motion. This suggests that the key to generalization is training on a diverse combination of datasets with a wide range of object velocities.

Table 1. **Analysis on Cross-Domain Generalization.** We train Flow4D [15] on AV2, Waymo, and nuScenes and evaluate each dataset-specific model across datasets. We further break down performance by velocity speed buckets (meters / frame). We find that Flow4D (Waymo) nearly matches Flow4D (AV2)'s overall Dynamic Mean EPE on AV2 (0.199 vs. 0.192, shown in green), and outperforms it on fast-moving objects (0.098 vs. 0.103, shown in gray). This suggests that Flow4D (Waymo) can *already* generalize across datasets. Flow4D (nuScenes) performs considerably worse on out-of-distribution datasets (shown in red) due its limited number of training examples.

Train	Test	FD (cm) ↓	Dyn. Mean ↓	[0, 0.5)	[0.5, 1.0)	[1.0, 2.0)	$[2.0,\infty)$
	AV2	8.55	0.192	0.020	0.119	0.114	0.103
AV2	Waymo	8.31	0.236	0.016	0.077	0.079	0.350
	nuScenes	20.40	0.463	0.017	0.249	0.334	0.610
	AV2	8.90	0.199	0.021	0.119	0.125	0.098
Waymo	Waymo	4.58	0.215	0.007	0.064	0.051	0.130
	nuScenes	16.04	0.408	0.017	0.217	0.319	0.540
	AV2	16.08	0.357	0.039	0.239	0.272	0.395
nuScenes	Waymo	17.24	0.364	0.022	0.222	0.209	0.598
	nuScenes	7.97	0.230	0.018	0.100	0.109	0.370

Towards Zero-Shot LiDAR Scene Flow. We argue that scaling up LiDAR-based scene flow methods will be a key enabler for 3D motion understanding and dynamic reconstruction in diverse environments. To this end, we retrain state-of-the-art methods on supervised data from AV2, Waymo, and nuScenes and demonstrate significant improvements for both in-distribution and out-ofdistribution generalization. We denote models trained with multiple datasets as UniFlow. To the best of our knowledge, UniFlow is the first to demonstrate the benefits of cross-domain training for LiDAR scene flow. Further, Uni-Flow models demonstrate remarkable zero-shot accuracy on TruckScenes [6], outperforming prior dataset-specific models by 30.1% (Table 6). Lastly, we find that crossdomain training on near-range (i.e  $\leq$  35 meters from the ego-vehicle) points improves scene flow generalization to unseen far-range points (Table 7). Intuitively, sparse LiDAR points near the ego-vehicle mimic the distribution of dense LiDAR points far away from the vehicle [28].

Why Does Multi-Dataset Training Work? Our experiments suggest that multi-dataset training improves LiDAR scene flow performance because scene flow is inherently

class-agnostic. This allows us to avoid complications arising from dataset-specific label definitions (Table 8). For example, nuScenes defines bicycle as excluding the rider, while Waymo includes the rider [25, 29]. Such label ambiguity poses a significant challenge for semantic tasks, potentially explaining why prior LiDAR-based semantic tasks like 3D object detection and semantic segmentation do not benefit from training on multiple datasets. Furthermore, we find that with careful augmentations, we can simulate diverse sensor configurations that improve cross-dataset generalization (Figure 4). For example, dropping out LiDAR beams from a Waymo point cloud makes the data look more like a point cloud from AV2 or nuScenes, while augmenting the height of a point cloud makes a sensor mounted on a sedan look like it was mounted on a truck.

**Contributions.** We present three major contributions. First, we highlight that dataset-specific scene flow models *already* show signs of cross-domain generalization, motivating our investigation into multi-dataset training. Next, we demonstrate that re-training existing scene flow methods on diverse, large-scale data yields state-of-the-art performance on nuScenes and Waymo, improving over our baselines by 35.2% and 5.1% respectively. Finally, we show that UniFlow outperforms dataset-specific models by 30.1% on TruckScenes, challenging conventional wisdom on LiDAR-based cross-domain generalization.

#### 2. Related Work

**Scene Flow Estimation** is the task of describing the 3D motion field between temporally successive point clouds [12, 37, 49], and is an important primitive for 3D motion understanding and dynamic scene reconstruction [39]. Early approaches [17, 42, 43, 50] learned point-wise features to estimate per-point flow but struggled to scale to large outdoor environments [35, 46]. More recent work [9, 13, 15, 24, 35] jointly estimates flow for all points in a scene. Contemporary methods can be broadly classified into feedforward models and optimization-based methods. Feedforward models directly learn a mapping between point cloud pairs and flow fields, but require large-scale human annotations [11, 15]. For real world datasets (typically from the autonomous vehicle domain), these human annotations are provided in the form of 3D bounding boxes and tracks for every object in the scene. In contrast, optimization-based methods do not require labeled data, and instead optimize a learned representation per-scene [18, 19]. This per-scene optimization is prohibitively expensive, making it difficult to scale to large datasets. For example, EulerFlow [36] achieves state-of-the-art unsupervised accuracy on many popular AV datasets, but takes over 24 hours to optimize each scene. In summary, feedforward models achieve efficient inference but demonstrate limited generalization beyond their training data, while optimization-based methods produce high quality flow for diverse scenes, but are too slow for real-time applications. Our work aims to reconcile this trade-off by training a single feedforward model that achieves robust generalization across diverse datasets and sensors.

Cross-Domain Generalization for LiDAR is a longstanding challenge in LiDAR-based perception. works in 3D object detection [7, 26] and semantic segmentation [2, 14, 45] show that models trained on multiple datasets often perform worse than dataset-specific models. This performance drop can be largely attributed to diverse sensor hardware (e.g., number of beams, scan pattern, point cloud density), environmental conditions (e.g., weather, geography), and sensor placement across datasets. To address these challenges, several methods have introduced data augmentation strategies [32], such as random point dropping [38] and object scaling [3], while others [23, 27] have proposed unsupervised domain adaptation techniques that align feature distributions across datasets. However, such data augmentation strategies primarily address the geometric domain gap between datasets. For motion-centric tasks such as scene flow, we argue that understanding the distribution of object velocities between datasets represents a critical yet overlooked axis for addressing cross-domain generalization. To this end, our work presents the first systematic study of this velocity domain gap.

# 3. UniFlow: Towards Zero-Shot LiDAR Scene Flow for Autonomous Vehicles

UniFlow aims to learn general motion priors that transfer to diverse and unseen LiDAR sensors by training a single scene flow model across diverse autonomous driving datasets. In this section, we describe the process of unifying four popular AV datasets and our training strategy.

Dataset Unification. We unify four widely used AV datasets to facilitate multi-dataset training. Importantly, we standardize LiDAR sensor frame rates and annotation frequencies to ensure that the time interval between LiDAR sweeps is consistent across datasets. This step is crucial because state-of-the-art scene flow methods parameterize motion as the displacement between two consecutive Li-DAR frames. Specifically, we down-sample high-frequency datasets like nuScenes (which provides LiDAR sweeps at 20 Hz) to 10 Hz to match AV2 and Waymo. For datasets with sparse scene flow annotations (e.g., nuScenes annotates tracks at 2 Hz), we train solely on the annotated frames and their real adjacent scans. This ensures that we do not introduce any label noise or motion artifacts due to interpolation. Lastly, we apply LineFit [8] for ground point removal for all datasets.

Unified Multi-Dataset Training. We retrain existing state-of-the-art scene flow architectures (SSF [13], Flow4D [15], and  $\Delta$ Flow [49]) on the unified dataset mixture of

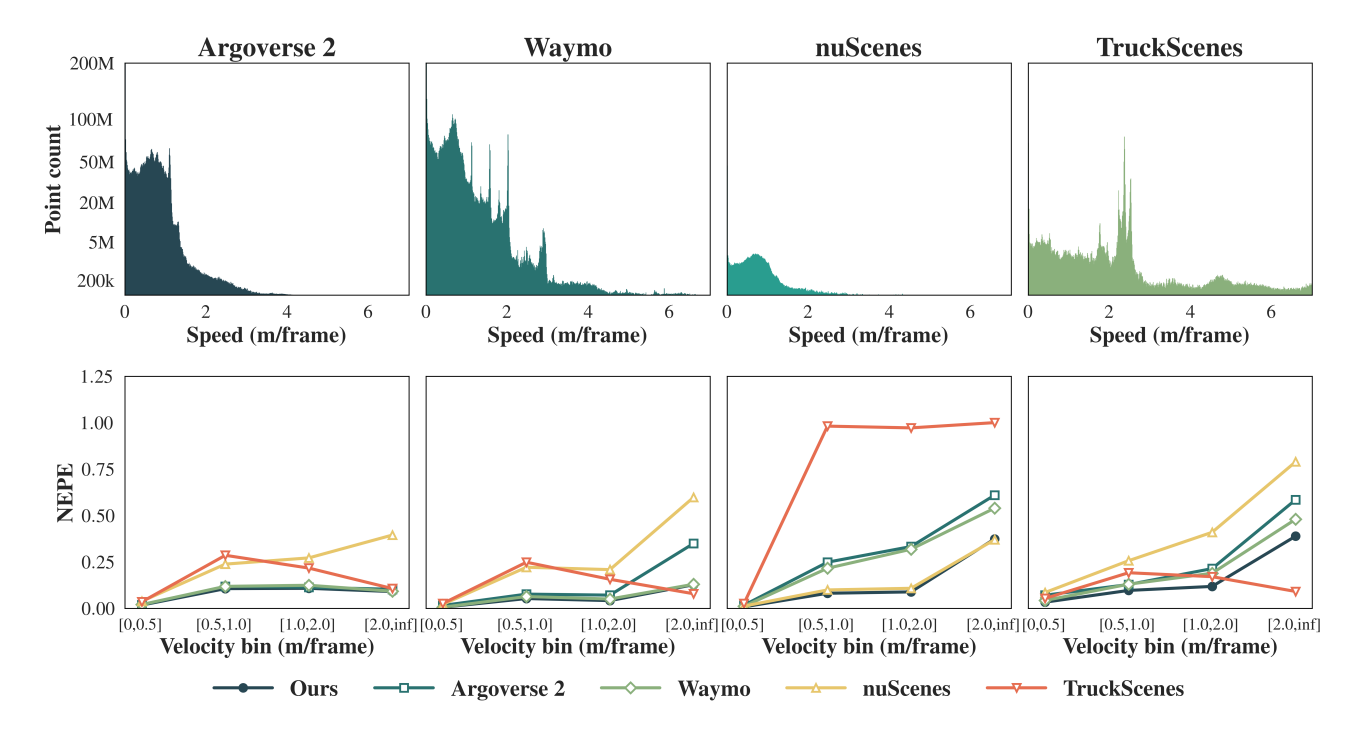


Figure 2. Cross-Dataset Generalization Correlates with Velocity Distribution. We plot the velocity distributions for the AV2, Waymo, nuScenes, and TruckScenes train sets (top) and the Dynamic Mean EPE per velocity bin of Flow4D trained on AV2, Waymo, nuScenes, TruckScenes, and UniFlow (bottom). Notably, Flow4D trained on TruckScenes outpeforms Flow4D trained on any other dataset for fast moving objects  $(2.0, \infty)$  across all datasets because it has the largest number of fast moving objects.

nuScenes, AV2, and Waymo. Importantly, we do not reweight dataset frequencies or apply dataset-specific augmentations. Instead, we employ a minimal yet effective augmentation set including height randomization to account for sensor placement and LiDAR ray dropping to simulate varying LiDAR point densities. This unified training paradigm encourages models to learn domain-agnostic geometric priors rather than memorizing dataset-specific motion patterns, resulting in significant zero-shot generalization improvements.

#### 4. Experiments

**Datasets.** We train and evaluate UniFlow on four largescale autonomous driving datasets to rigorously evaluate cross-domain generalization to diverse sensor configura-

Table 2. **Dataset Statistics.** We summarize the four datasets used for training and evaluation below. We include both the (# Total Frames / # Annotated Frames) for nuScenes and TruckScenes.

Dataset	Split	# Scenes	# Frames	LiDAR Setup	Ego-Vehicle	Scenario
Argoverse 2	Train Val	700 150	110,071 23,547	2 x 32-beam	Car	Urban / City
Waymo	Train Val	798 202	155,000 40,000	1 x 64-beam	Car	Urban / Suburban
nuScenes	Train Val	700 150	137,575 / 27,392 29,126 / 5,798	1 x 32-beam	Car	Urban / City
TruckScenes	Train Val	524 75	101,902 / 20,380 14,625 / 2,925	2 x 64-beam	Truck	Highway

tions, ego-vehicle platforms, and driving scenarios (Table 2). AV2 and nuScenes collect data in dense urban environments with 32-beam LiDARs. Waymo uses a custom Li-DAR sensor to collect denser point clouds from urban and suburban environments with more varied driving dynamics. We evaluate zero-shot generalization using TruckScenes [6] since it collects data in different environments (high-speed highway scenes vs. urban and suburban scenes), with different sensors (32-beam LiDARs vs. 64-beam LiDARs), using a different vehicle type (truck vs. sedan). These four datasets allow us to systematically analyze the impact of point density (32-beam vs. 64-beam), ego-vehicle perspective (car vs. truck), and velocity (urban vs. highway) on cross-domain generalization.

Metrics. We use *Dynamic Bucket-Normalized EPE* [12] as our primary metric to evaluate cross-domain generalization, particularly across diverse velocity distributions. This protocol is specifically designed to be both class-aware and speed-normalized. By normalizing motion estimation error by an object's speed, Dynamic Bucket-Normalized EPE measures the fraction of motion *not* described, enabling fair comparison between slow-moving pedestrians and fast-moving vehicles. We also report Three-Way EPE [4] for completeness, but note that it is a biased estimator of performance.

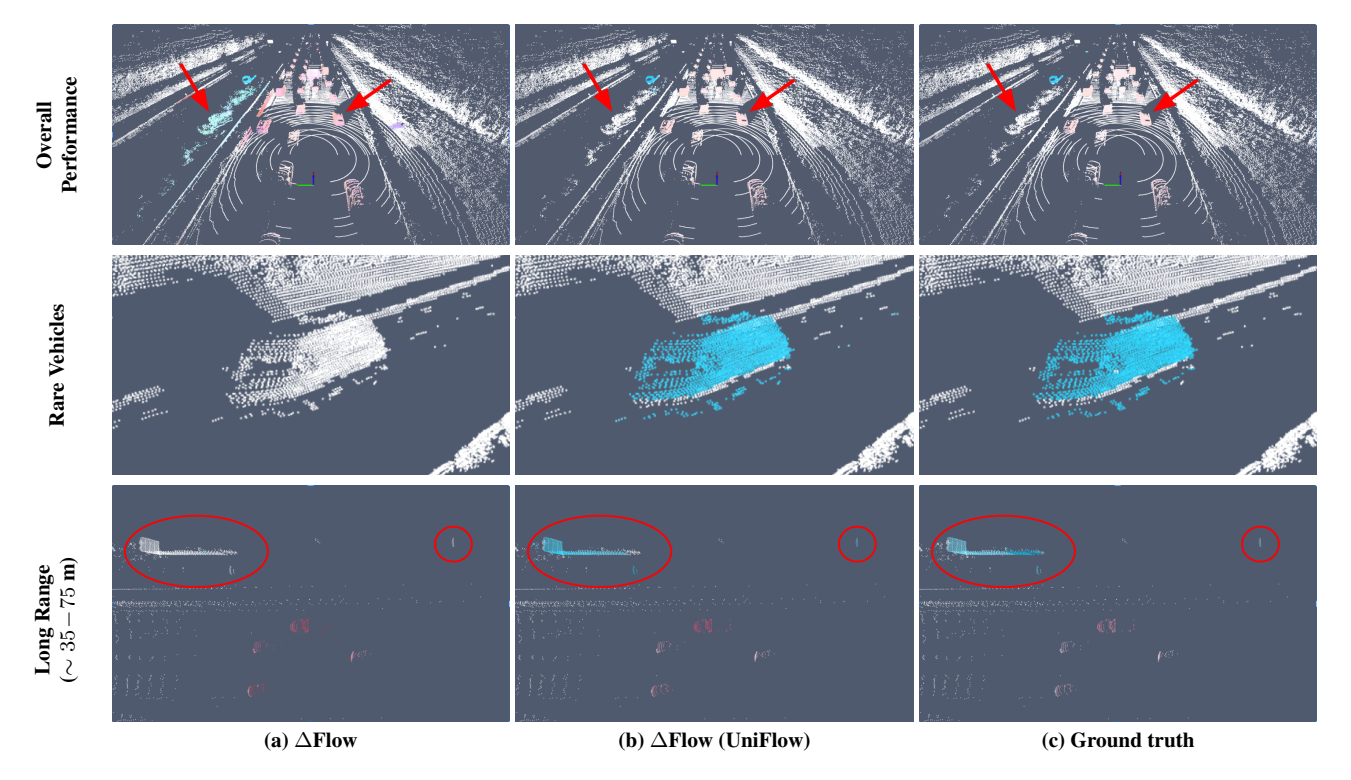


Figure 3. **Zero-Shot Generalization on TruckScenes.** We qualitatively compare the dataset-specific  $\Delta$ Flow model and our  $\Delta$ Flow (UniFlow) model above.  $\Delta$ Flow (UniFlow) produces more accurate vehicle motion estimates in general, and avoids falsely predicting motion for rain artifacts (on the top left) as seen in  $\Delta$ Flow (top row). Next,  $\Delta$ Flow (UniFlow) correctly estimates the motion of the van since it has been trained on more examples of rare classes (middle row). Lastly,  $\Delta$ Flow (UniFlow) generalizes significantly better at long-range, accurately estimating the truck's motion at  $\sim$ 35 m and the car's motion at  $\sim$ 70 m, despite extreme point sparsity (bottom row).

**Baselines.** We compare UniFlow against both self-supervised and fully-supervised methods: NSFP [18], FastNSF [19], ICPFlow [21], SeFlow [47], SeFlow++ [48], EulerFlow [36], VoteFlow [22], TrackFlow [12], DeFlow [46], SSF [13], Flow4D [15] and  $\Delta$ Flow [49]. To ensure fairness, Argoverse 2 test-set results are obtained directly from the public leaderboard. We use Waymo, nuScenes and TruckScenes baselines as implemented in OpenSceneFlow with standard training hyperparameters.

Comparison to State-of-the-Art Methods. We demonstrate the effectiveness of the UniFlow framework by retraining SSF, Flow4D, and  $\Delta$ Flow on multiple datasets and compare their performance against recent approaches on popular scene flow benchmarks (Tables 3, 4, and 5). On the Argoverse 2 test set, Flow4D (UniFlow) improves over Flow4D by 8.97% and SSF (UniFlow) improves over SSF by 13.81% in Dynamic Mean EPE. Moreover, Flow4D (UniFlow) achieves near-parity with EulerFlow at a fraction of the runtime. We see similar improvements between Flow4D and SSF and their UniFlow counterparts on the Waymo (Table 4) and nuScenes (Table 5) validation sets. Interestingly, SSF (UniFlow) outperforms Flow4D (Uni-

Table 3. **Argoverse 2 Test Set.** We compare UniFlow with recent methods on the Argoverse 2 test set. Notably, Flow4D (UniFlow) outperforms Flow4D by 11.41%, while SSF (UniFlow) outperforms SSF by 17.89% Dynamic Mean EPE. Notably,  $\Delta$ Flow (UniFlow) achieves slightly worse mean Dynamic EPE that  $\Delta$ Flow. This suggests that performance on AV2 may be saturating, and further improvements may be overfitting to label noise.

M-41 1-	Thre	e-way F	PE (cn	1) ↓	D	ynamic	Bucket-N	ormalized	<b></b>
Methods	Mean	FD	FS	BS	Mean	Car	Other	Pedestr.	VRU
Unsupervised									
NSFP	6.06	11.58	3.16	3.44	0.422	0.251	0.331	0.722	0.383
FastNSF	11.18	16.34	8.14	9.07	0.383	0.296	0.413	0.500	0.322
SeFlow	4.86	12.14	1.84	0.60	0.309	0.214	0.291	0.464	0.265
ICP Flow	6.50	13.69	3.32	2.50	0.331	0.195	0.331	0.435	0.363
EulerFlow	4.23	4.98	2.45	5.25	0.130	0.093	0.141	0.195	0.093
Supervised									
TrackFlow	4.73	10.30	3.65	0.24	0.269	0.182	0.305	0.358	0.230
DeFlow	3.43	7.32	2.51	0.46	0.276	0.113	0.228	0.496	0.266
SSF	2.73	5.72	1.76	0.72	0.181	0.099	0.162	0.292	0.169
Flow4D	2.24	4.94	1.31	0.47	0.145	0.087	0.150	0.216	0.127
$\Delta$ Flow	2.11	4.33	1.37	0.64	0.113	0.077	0.129	0.149	0.096
SSF (UniFlow, Ours)	2.23	4.89	1.31	0.51	0.156	0.102	0.147	0.241	0.134
Flow4D (UniFlow, Ours)	2.07	4.50	1.31	0.40	0.132	0.072	0.131	0.218	0.107
$\Delta$ Flow (UniFlow, Ours)	2.07	4.41	1.26	0.54	0.118	0.073	0.136	0.164	0.098

Flow) on nuScenes, suggesting that the SSF architecture is naturally better suited for processing sparse point clouds.

**TruckScenes Zero-Shot Performance.** We demonstrate UniFlow's strong zero-shot generalization capabilities with extensive evaluations on TruckScenes (Table 6).

https://github.com/KTH-RPL/OpenSceneFlow

Table 4. Waymo Validation Set. We compare UniFlow with recent methods on Waymo val. Notably, supervised methods achieve significantly lower EPE than unsupervised methods, with  $\Delta$ Flow (UniFlow) beating SeFlow by 61.99% on Foreground Dynamic.

Methods	Thr	ee-way l	EPE (cm	ı) ↓	Dynar	nic Bucl	ket-Normal	ized ↓
Methods	Mean	FD	FS	BS	Mean	Car	Pedestr.	VRU
Unsupervised								
NSFP	10.05	17.12	10.81	2.21	0.574	0.315	0.823	0.584
ZeroFlow	8.64	22.40	1.57	1.96	0.770	0.444	0.982	0.884
SeFlow	8.50	20.81	2.14	2.57	0.328	0.305	0.485	0.185
SeFlow++	3.63	9.30	0.87	0.71	0.232	0.201	0.521	0.247
Supervised								
DeFlow	4.46	9.80	2.59	0.98	-	-	-	-
SSF	2.19	5.62	0.74	0.23	0.264	0.097	0.469	0.225
Flow4D	1.82	4.58	0.61	0.28	0.215	0.074	0.423	0.146
$\Delta$ Flow	1.40	3.27	0.58	0.35	0.198	0.073	0.407	0.114
SSF (UniFlow, Ours)	1.85	4.74	0.58	0.22	0.234	0.075	0.434	0.195
Flow4D (UniFlow, Ours)	1.60	3.83	0.68	0.30	0.191	0.064	0.400	0.110
ΔFlow (UniFlow, Ours)	1.38	3.07	0.61	0.46	0.188	0.065	0.403	0.096

Table 5. **nuScenes Validation Set.** We compare UniFlow with recent methods on the nuScenes val set. Interestingly, SSF (UniFlow) outperforms Flow4D (UniFlow) by 26.53% Dynamic Mean EPE, suggesting that SSF's architecture more effectively learns to estimate flow from sparse point clouds.

M. a. 1	Thr	ee-way I	EPE (cr	n) ↓	D	ynamic	Bucket-N	ormalized	<b>+</b>
Methods	Mean	FD	FS	BS	Mean	Car	Other	Pedestr.	VRU
Unsupervised									
NSFP	10.79	20.26	4.88	7.23	0.602	0.463	0.456	0.829	0.662
FastNSF	12.16	18.20	6.11	12.18	0.560	0.436	0.523	0.737	0.543
SeFlow	8.19	16.15	3.97	4.45	0.554	0.396	0.635	0.726	0.419
Supervised									
DeFlow	3.98	6.99	3.45	1.50	0.314	0.163	0.286	0.533	0.275
SSF	3.00	6.55	2.04	0.41	0.220	0.142	0.197	0.398	0.144
Flow4D	3.46	7.97	1.85	0.55	0.230	0.160	0.241	0.345	0.176
$\Delta$ Flow	2.33	4.83	1.37	0.79	0.216	0.138	0.219	0.327	0.181
SSF (UniFlow, Ours)	1.97	4.33	1.38	0.20	0.144	0.081	0.131	0.267	0.097
Flow4D (UniFlow, Ours)	3.01	7.28	1.47	0.28	0.196	0.137	0.219	0.272	0.157
ΔFlow (UniFlow, Ours)	1.63	3.19	1.29	0.42	0.140	0.098	0.137	0.232	0.091

Table 6. **TruckScenes Validation Set.** We compare UniFlow with recent methods on the TruckScenes val set. According to Three-Way EPE, Flow4D achieves the best performance due to low Foreground Dynamic error. However, Dynamic Bucket Normalized EPE highlights that Flow4D (UniFlow) outperforms it across all moving object categories, most notably on pedestrians and VRUs. This reinforces that Three-Way EPE is a biased metric.

Methods	Thi	ee-way E	PE (cn	ı) ↓	D	ynamic	Bucket-N	ormalized	<b></b>
Methous	Mean	FD	FS	BS	Mean	Car	Other	Pedestr.	VRU
Unsupervised									
NSFP	45.63	120.45	2.07	14.38	0.658	0.303	0.350	1.221	0.758
FastNSF	30.72	59.44	3.35	29.38	0.588	0.218	0.376	1.124	0.635
SeFlow	37.41	103.97	1.56	6.68	0.681	0.494	0.752	0.886	0.591
ICP Flow	58.82	169.91	1.43	5.12	0.472	0.302	0.614	0.596	0.376
Supervised									
DeFlow	7.30	16.47	1.67	3.77	0.570	0.180	0.410	0.970	0.730
SSF	6.20	15.17	1.01	2.44	0.453	0.215	0.308	0.875	0.414
Flow4D	16.14	44.87	1.71	1.85	0.456	0.176	0.351	0.885	0.413
$\Delta$ Flow	7.28	16.26	1.36	4.52	0.402	0.196	0.400	0.690	0.323
Zero-shot									
SSF (UniFlow, Ours)	35.23	103.72	1.69	0.27	0.435	0.149	0.455	0.669	0.466
Flow4D (UniFlow, Ours)	23.59	68.41	1.78	0.57	0.281	0.088	0.277	0.530	0.230
$\Delta$ Flow (UniFlow, Ours)	15.76	45.76	1.02	1.32	0.283	0.101	0.293	0.513	0.226

All baseline methods (except UniFlow) were trained on TruckScenes. Despite never being explicitly trained on high speed highway scenes, Flow4D (UniFlow) significantly outperforms the dataset-specific Flow4D on Dynamic Mean EPE. Notably, Flow4D (UniFlow) was only trained on urban driving scenes collected from a sedan, indicating that our approach can successfully generalize across significant domain gaps. Table 6 also highlight the impor-

Table 7. **Ablation on Long-Range Generalization.** All  $^{\rm LR}$  results are obtained by evaluating models at extended voxel ranges while keeping the voxel size fixed and reusing the original trained weights.  $^{\rm ZS}$  denotes zero-shot evaluation, where the model has never seen the target domain during training. We report Dynamic Mean EPE for each distance interval from the ego-vehicle.  $\Delta Flow$  (UniFlow) demonstrates strong zero-shot generalization to extended spatial ranges for both in-domain and out-of-domain datasets.

Dataset	Method	Mean	0-35	35-50	50-75	75-100	100-inf
	ΔFlow	0.526	0.117	0.492	0.745	0.708	0.568
AV2	$\Delta Flow^{LR}$	0.259	0.117	0.205	0.240	0.325	0.409
	ΔFlow <sup>LR</sup> (UniFlow, Ours)	$0.226_{\downarrow 12.7\%}$	$0.114_{\downarrow 2.6\%}$	$0.198_{\downarrow 3.4\%}$	$0.219_{\downarrow 8.8\%}$	$0.260_{\downarrow 20.0\%}$	$0.339_{\downarrow 17.1\%}$
	$\Delta$ Flow	0.379	0.055	0.455	0.628	-	-
Waymo	$\Delta Flow^{LR}$	0.115	0.068	0.112	0.166	-	-
	∆Flow <sup>LR</sup> (UniFlow, Ours)	$0.105_{\downarrow 9.1\%}$	$0.063_{\downarrow 7.4\%}$	$0.104_{\downarrow 7.1\%}$	$0.149_{\downarrow 10.2\%}$	-	-
	$\Delta$ Flow	0.389	0.172	0.380	0.633	0.606	-
nuScenes	$\Delta Flow^{LR}$	0.267	0.181	0.242	0.318	0.447	-
	ΔFlow <sup>LR</sup> (UniFlow, Ours)	$0.248_{\downarrow 7.1\%}$	$0.166_{\downarrow 7.9\%}$	$0.209_{\downarrow 13.6\%}$	$0.301_{\downarrow 5.3\%}$	$0.405_{\downarrow 9.4\%}$	-
	ΔFlow	1.679	1.211	1.514	1.901	1.835	1.936
TruckScenes	$\Delta$ Flow <sup>LR</sup>	1.479	1.184	1.311	1.487	1.582	1.831
	ΔFlow <sup>LR,ZS</sup> (UniFlow, Ours)	$0.880_{\pm 40.6\%}$	$0.786_{\downarrow 33.6\%}$	$0.826_{\pm 37.0\%}$	$0.694_{\downarrow 53.3\%}$	$0.779_{\downarrow 50.8\%}$	1.317,28,1%

tance of the speed normalized and bucketed EPE metric [12], as Threeway-EPE results don't adequately measure Flow4D's (UniFlow) significant improvements on pedestrian and VRU performance.

Analysis of Long-Range Generalization. To evaluate whether unified training produces range-robust representations, we evaluate how models trained on short-range Li-DAR data transfer to longer-range settings without retraining. Specifically, we extend the voxelization range during inference while keeping the voxel size identical to the original trained model. This change alters only the spatial coverage of the dynamic voxelization module, requiring a simple weight transfer step to adapt to the new grid dimensions while preserving all learned features. As shown in Table 7, UniFlow<sup>LR</sup> consistently outperforms  $\Delta$ Flow<sup>LR</sup> across all distance intervals on AV2, reducing Dynamic Mean EPE by 12.7% on average and up to 20.0% in the 75-100 m range. This indicates that unified multi-dataset training produces representations that remain robust even when the perception range is significantly expanded. On TruckScenes, UniFlow<sup>LR,ZS</sup> achieves a remarkable 40.6% reduction in overall error compared to  $\Delta Flow^{LR}$ , with improvements exceeding 50% in the 50–100 m range, despite never being trained on this dataset. These results highlight that the representations learned through unified multi-dataset training naturally scale to larger spatial extents.

#### 4.1. Ablation Studies

Analysis of Semantic Cross-Domain Generalization. We evaluate the benefits unified training on both geometric and semantic understanding by extending Flow4D with a multitask semantic head. This new Flow4D variant simultaneously predicts scene flow and per-point semantics using the same backbone features. Since all datasets follow different taxonomies, we map their annotations to four coarse categories (e.g. car, other, pedestrian, and VRU) and jointly train the model with an additional class-balanced

Table 8. Ablation on Semantic Cross-Domain Generalization. We validate our claim that semantics less generalizable than motion by retraining Flow4D with an additional per-point semantic classification head. Notably, training Flow4D on the unified dataset improves zero-shot scene flow estimation on TruckScenes, but hinders mIoU on out-of-distribution datasets.

Dat	Dataset Scene Flow↓		Semantic Classification ↑							
Train	Test	3-Way (cm)	Dyn. Norm.	mIoU	Accuracy	CAR	OTHER	PED	VRU	
AV2	AV2	3.46	0.204	75.3%	93.9%	90.9%	86.2%	88.2%	36.0%	
Waymo	Waymo	1.74	0.202	79.1%	98.9%	99.0%	-	87.1%	51.3%	
nuScenes	nuScenes	2.99	0.214	70.5%	89.8%	82.8%	83.3%	80.5%	35.4%	
TruckScenes	TruckScenes	15.56	0.462	64.6%	95.3%	91.0%	92.9%	32.6%	42.1s%	
Unified	AV2	3.26	0.178	78.8%	94.2%	91.4%	85.8%	90.0%	47.9%	
Unified	Waymo	1.57	0.190	64.0%	99.4%	99.4%	0.0%	93.1%	63.5%	
Unified	nuScenes	3.19	0.215	79.9%	93.4%	88.0%	89.1%	82.3%	60.3%	
Unified	TruckScenes	24.69	0.288	40.5%	66.1%	53.5%	46.4%	20.1%	41.9%	

Table 9. **Ablation on TruckScenes.** We ablate the impact of multi-dataset training, data augmentation, and model scaling on zero-shot TruckScenes performance. All the model architectures we test benefit from multi-dataset training, while data augmentation continues to provide notable improvements even with  $3 \times 10^{-2}$  larger training sets, suggesting that scaling up UniFlow may yield further improvements.

Method	FD (cm) ↓	Dynamic EPE $\downarrow$	[0, 0.5)	[0.5, 1.0)	[1.0, 2.0)	[2.0, ∞)
Flow4D	116.01	0.336	0.071	0.129	0.215	0.586
+ Unified Dataset	93.76 \(\pmu22.25\)	$0.310_{\ \downarrow 0.026}$	$0.040_{\downarrow 0.031}$	$0.116_{\downarrow 0.013}$	$0.170_{\downarrow 0.045}$	$0.594_{0.008}$
+ Augmentation	68.32 425.44	0.301 10.009	0.047 10.007	$0.111_{\pm 0.005}$	$0.141_{\pm 0.029}$	$0.407_{\pm 0.187}$
+ XL Backbone	68.41 <sub>↑0.09</sub>	0.281 10.020	$0.033_{\ \downarrow 0.014}$	$0.097_{\ \downarrow 0.014}$	$0.119_{\downarrow 0.022}$	$0.389_{\ \downarrow 0.018}$
SSF	170.65	0.737	0.049	0.555	0.740	0.971
+ Unified Dataset	133.04 137.61	0.577 <sub>↓0.160</sub>	$0.042_{\pm 0.007}$	$0.257_{\pm 0.298}$	$0.514_{\pm 0.226}$	$0.827_{\pm 0.144}$
+ Augmentation	103.72 \$\pmu_29.32\$	0.435 \(\psi_{0.142}\)	$0.036_{\downarrow 0.006}$	$0.149_{\ \downarrow 0.108}$	$0.285_{\ \downarrow 0.229}$	$0.637_{\downarrow 0.190}$
$\Delta$ Flow	117.83	0.357	0.067	0.114	0.302	0.714
+ Unified Dataset	84.16 \(\pmu_{33.67}\)	0.331 \(\pi_{0.026}\)	$0.036_{\downarrow 0.031}$	0.119 0.005	$0.268_{\pm 0.034}$	$0.659_{\pm 0.055}$
+ Augmentation	15.76 ↓68.40	0.283 40.048	$0.039_{\ \uparrow 0.003}$	$0.094_{\ \downarrow 0.025}$	$0.127_{\ \downarrow 0.141}$	$0.429_{\ \downarrow 0.230}$

cross-entropy loss. As shown in Table 8, adding the semantic head has almost no effect on scene flow accuracy, indicating that the auxiliary task does not interfere with motion estimation. Consistent with our original findings, unified multi-dataset training continues to improve both indomain and zero-shot performance for scene flow. However, training the semantic prediction head on the unified dataset yields mixed results. Models trained on unified datasets show small in-domain gains, but perform substantially worse than dataset-specific model when evaluated on unseen domains. This supports our hypothesis that dataset unification primarily benefits low-level geometric representations, while high-level semantics remain sensitive to dataset-specific biases.

Analysis of Training Recipe. We ablate the impact of multi-dataset training, data augmentation, and model scaling on zero-shot TruckScenes performance in Table 9. All baselines are trained on Waymo only to ensure zero-shot evaluation. All model architectures show clear gains from multi-dataset training. Notably, despite training on a dataset three times larger, data augmentation continues to show substantial improvements, indicating that further scaling may yield additional performance gains.

Analysis on Dataset Weighting Strategies. We further examine the impact of per-dataset sampling frequencies on our unified training approach. All models are trained on the unified dataset for a fixed number of iterations, but we vary

Table 10. **Ablation on Dataset Weighting Strategies.** We retrain Flow4D (UniFlow) while varying the sampling frequency of data from each domain. Unified training consistently outperforms single-domain baselines, even if the in-domain dataset is only sampled 5% of the time. Somewhat unsurprisingly, one can maximize in-domain performance by slightly biasing sampling towards indomain data.

Weight Strategy	Dataset Weights	Mean	FD	FS	BS	Dynamic M
TruckScenes						
Proportional	60%W, 25%A, 15%N	23.59	68.41	1.78	0.57	0.281
Uniform	33%W, 33%A, 33%N	30.44	89.01	1.73	0.58	0.307
Waymo Heavy	90%W, 5%A, 5%N	33.25	97.48	1.72	0.56	0.312
AV2 Heavy	90%A, 5%W, 5%N	29.82	87.08	1.70	0.67	0.310
nuScenes Heavy	90%N, 5%A, 5%W	31.26	91.11	1.70	0.96	0.332
Argoverse 2						
Proportional	60%W, 25%A, 15%N	3.24	7.83	1.26	0.63	0.176
Uniform	33%W, 33%A, 33%N	3.22	7.79	1.25	0.63	0.176
Waymo Heavy	90%W, 5%A, 5%N	3.28	7.87	1.28	0.69	0.189
AV2 Heavy	90%A, 5%W, 5%N	3.21	7.80	1.27	0.56	0.183
nuScenes Heavy	90%N, 5%A, 5%W	3.51	8.42	1.37	0.75	0.192
AV2-only	100%A	3.62	8.55	1.62	0.69	0.192
nuScenes						
Proportional	60%W, 25%A, 15%N	3.01	7.28	1.47	0.28	0.196
Uniform	33%W, 33%A, 33%N	2.07	4.70	1.34	0.16	0.134
Waymo Heavy	90%W, 5%A, 5%N	2.87	6.88	1.48	0.25	0.199
AV2 Heavy	90%A, 5%W, 5%N	2.93	6.93	1.55	0.30	0.222
nuScenes Heavy	90%N, 5%A, 5%W	1.75	3.81	1.29	0.15	0.109
nuScenes-only	100%N	3.46	7.97	1.85	0.55	0.230
Waymo						
Proportional	60%W, 25%A, 15%N	1.60	3.83	0.68	0.30	0.191
Uniform	33%W, 33%A, 33%N	1.59	3.89	0.61	0.27	0.195
Waymo Heavy	90%W, 5%A, 5%N	1.50	3.75	0.55	0.21	0.203
AV2 Heavy	90%A, 5%W, 5%N	1.81	4.41	0.70	0.32	0.213
nuScenes Heavy	90%N, 5%A, 5%W	1.90	4.76	0.61	0.32	0.215
Waymo-only	100%W	1.82	4.58	0.61	0.28	0.215

the per-domain sampling frequency to control how often samples from each distribution are drawn. As shown in Table 10, unified training consistently outperforms the single-dataset baselines, even under extreme weighting schemes. For example, on nuScenes, models trained with only 5% exposure to the target domain and 90% exposure to a very different distribution (Waymo) still surpass the in-domain baseline by 13.5% on Dynamic Mean EPE, indicating that even limited cross-domain exposure provides considerable benefits. Unsurprisingly, one can maximize in-domain performance by slightly biasing the model twoards in-domain data. Lastly, we find that uniformly sampling all datasets with equal probability yields the best out-of-distribution performance on TruckScenes.

Analysis on Scaling Laws. We evaluate Flow4D (Uni-Flow) with varying amounts of training data on both indistribution benchmarks (AV2, nuScenes, and Waymo) and an out-of-distribution benchmark (TruckScenes) in Fig 4. As expected, larger training sets reduce Dynamic Mean EPE. However, data augmentation proves far more critical for out-of-distribution performance, while its effect on indistribution performance remains minimal.

Analysis on Frame-Rate. We evaluate the generalization of Flow4D (UniFlow), SSF (UniFlow) and  $\Delta$ Flow (UniFlow) across different frame rates in Table 11. Slower frame rates approximate a slower-moving ego-vehicle,

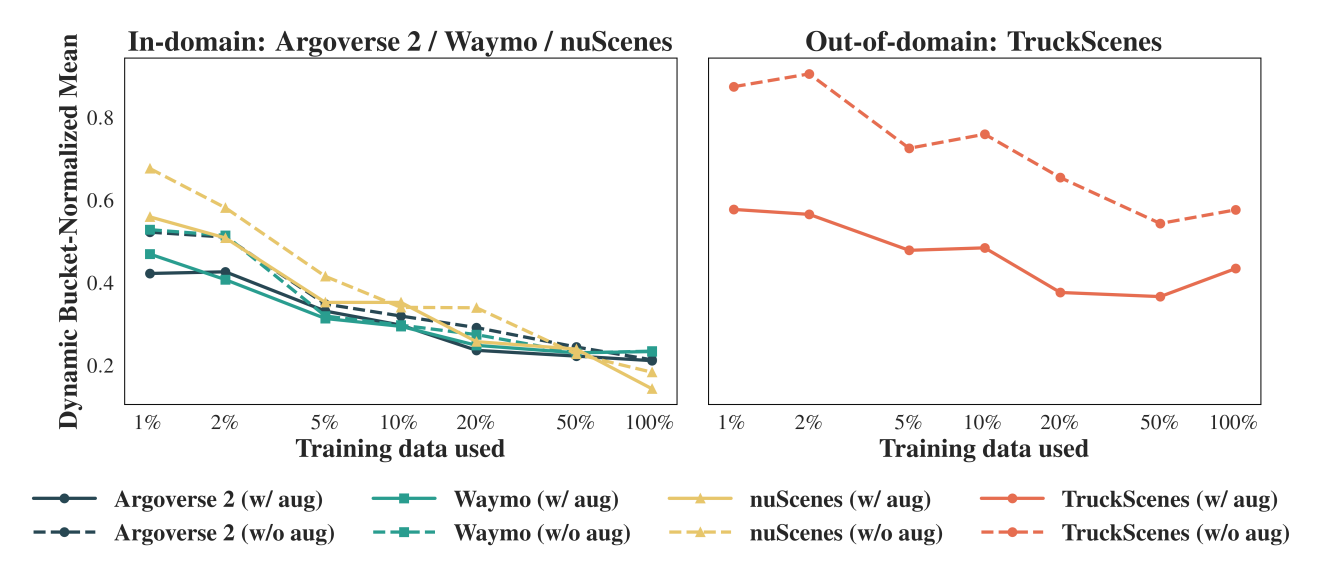


Figure 4. Scaling Laws. We evaluate both the in-distribution (on AV2, nuScenes, and Waymo) and out-of-distribution (on TruckScenes) performance of Flow4D (UniFlow) with different amounts of training data. Unsurprisingly, increasing data reduces Dynamic Mean EPE. However, we find that data augmentation is significantly more important for out-of-distribution performance, and has minimal impact on in-distribution performance. Lower is better.

Table 11. **Ablation on Frame-Rate.** We evaluate Flow4D (UniFlow), SSF (UniFlow) and  $\Delta$ Flow's (UniFlow) generalization to different frame rates. Note that slower frame-rates effectively mimic a slower ego-vehicle, while faster-frame rates mimic a faster ego-vehicle. Although we train all models on 10 Hz annotations, multi-dataset training yields better results, particularly at slower frame rates. Interestingly, faster frame rates do not negatively impact performance nearly as much as slower frame-rates.

			nn (						
Method		ee-way I					Bucket-No		
	Mean ↓	FD ↓	FS ↓	BS ↓	Dyn. Mean ↓	Car ↓	Other $\downarrow$	Pedestr. ↓	VRU ↓
2 Hz									
Flow4D	30.79	88.10	3.26	1.02	0.495	0.364	0.494	0.613	0.509
SSF	31.16	89.82	3.07	0.59	0.520	0.363	0.498	0.684	0.535
$\Delta$ Flow	26.41	74.43	3.12	1.66	0.457	0.370	0.471	0.545	0.440
Flow4D (UniFlow, Ours)	27.52	79.54	2.36	0.65	0.444	0.297	0.415	0.587	0.476
SSF (UniFlow, Ours)	28.67	83.11	2.50	0.39	0.503	0.296	0.432	0.671	0.611
ΔFlow (UniFlow, Ours)	23.87	68.26	2.46	0.88	0.398	0.306	0.420	0.494	0.494
5 Hz									
Flow4D	9.58	25.64	2.45	0.65	0.323	0.215	0.312	0.432	0.333
SSF	8.74	23.02	2.74	0.47	0.311	0.179	0.286	0.489	0.291
$\Delta$ Flow	6.43	16.54	1.98	0.76	0.264	0.173	0.271	0.369	0.242
Flow4D (UniFlow, Ours)	8.02	21.78	1.92	0.37	0.290	0.190	0.265	0.405	0.302
SSF (UniFlow, Ours)	6.75	17.96	2.06	0.22	0.285	0.135	0.218	0.454	0.333
ΔFlow (UniFlow, Ours)	5.26	13.44	1.81	0.58	0.232	0.150	0.220	0.343	0.214
10 Hz (Standard Frame Ro	ite)								
Flow4D	3.46	7.97	1.85	0.55	0.230	0.160	0.241	0.241	0.176
SSF	3.00	6.55	2.04	0.41	0.220	0.142	0.197	0.398	0.144
$\Delta$ Flow	2.05	4.19	1.36	0.59	0.173	0.132	0.184	0.261	0.117
Flow4D (UniFlow, Ours)	3.01	7.28	1.47	0.28	0.196	0.137	0.219	0.272	0.157
SSF (UniFlow, Ours)	1.97	4.33	1.38	0.20	0.144	0.081	0.131	0.267	0.097
ΔFlow (UniFlow, Ours)	1.63	3.18	1.29	0.42	0.140	0.098	0.137	0.232	0.091
20 Hz									
Flow4D	2.55	5.79	1.35	0.50	0.272	0.196	0.315	0.377	0.200
SSF	2.94	6.72	1.73	0.38	0.316	0.177	0.303	0.533	0.250
$\Delta$ Flow	1.60	3.28	0.48	0.48	0.220	0.167	0.231	0.327	0.156
Flow4D (UniFlow, Ours)	1.95	4.65	1.00	0.21	0.230	0.171	0.269	0.315	0.163
SSF (UniFlow, Ours)	2.13	5.16	1.11	0.12	0.246	0.127	0.275	0.395	0.189
ΔFlow (UniFlow, Ours)	1.30	2.60	0.96	0.34	0.010	0.153	0.215	0.277	0.138

while faster frame rates approximate a faster one. Although all models are trained using 10 Hz annotations, multi-dataset training consistently improves performance, especially at slower frame rates. Interestingly, higher frame rates have a smaller negative effect on performance, likely because models only need to estimate smaller displacement vectors for each timestep.

Limitations and Future Work. We investigate the domain gap between different LiDAR scene flow datasets and show that multi-dataset training enables strong generalization. Due to a lack of benchmarks and baselines in diverse domains, our experiments are limited to autonomous driving scenes. Future work should explore non-AV settings.

#### 5. Conclusion

In this paper, we introduce UniFlow, a frustratingly simple approach that re-trains off-the-shelf LiDAR scene flow models with diverse data from multiple datasets. Although prior work in LiDAR-based 3D object detection and segmentation don't seem to benefit from multi-dataset training, we posit that our proposed method works well "lowlevel" tasks such as motion estimation may be less sensitive to sensor configuration. Notably, our model establishes a new state-of-the-art Waymo and nuScenes, improving over prior work by 5.1% and 35.2% respectively. Although Uni-Flowis primarily trained on urban city driving scenarios, we demonstrate that it generalizes surprisingly well to highway truck driving without any dataset-specific fine-tuning. Our extensive analysis shows that such improvements are model-agnostic, suggesting that future scene flow methods should adopt a multi-dataset training strategy.

#### References

- [1] Holger Caesar, Varun Bankiti, Alex H. Lang, Sourabh Vora, Venice Erin Liong, Qiang Xu, Anush Krishnan, Yu Pan, Giancarlo Baldan, and Oscar Beijbom. nuscenes: A multimodal dataset for autonomous driving. In CVPR, 2020. 1
- [2] Andrew Caunes, Thierry Chateau, and Vincent Fremont. seg\_3d\_by\_pc2d: Multi-view projection for domain generalization and adaptation in 3d semantic segmentation. *arXiv* preprint arXiv:2505.15545, 2025. 3
- [3] Jun Cen, Peng Yun, Shiwei Zhang, Junhao Cai, Di Luan, Mingqian Tang, Ming Liu, and Michael Yu Wang. Openworld semantic segmentation for lidar point clouds. In *Eu*ropean Conference on Computer Vision, pages 318–334. Springer, 2022. 3
- [4] Nathaniel Chodosh, Deva Ramanan, and Simon Lucey. Reevaluating lidar scene flow. In *Proceedings of the IEEE/CVF Winter Conference on Applications of Computer Vision* (WACV), pages 6005–6015, 2024. 4
- [5] Alexey Dosovitskiy, Philipp Fischer, Eddy Ilg, Philip Hausser, Caner Hazirbas, Vladimir Golkov, Patrick Van Der Smagt, Daniel Cremers, and Thomas Brox. Flownet: Learning optical flow with convolutional networks. In *Proceedings of the IEEE international conference on computer vision*, pages 2758–2766, 2015.
- [6] Felix Fent, Fabian Kuttenreich, Florian Ruch, Farija Rizwin, Stefan Juergens, Lorenz Lechermann, Christian Nissler, Andrea Perl, Ulrich Voll, Min Yan, et al. Man truckscenes: A multimodal dataset for autonomous trucking in diverse conditions. Advances in Neural Information Processing Systems, 37:62062–62082, 2024. 2, 4
- [7] Deepti Hegde, Suhas Lohit, Kuan-Chuan Peng, Michael Jones, and Vishal Patel. Multimodal 3d object detection on unseen domains. In *Proceedings of the Computer Vision and Pattern Recognition Conference*, pages 2499–2509, 2025. 3
- [8] Michael Himmelsbach, Felix V Hundelshausen, and H-J Wuensche. Fast segmentation of 3d point clouds for ground vehicles. In *Intelligent Vehicles Symposium (IV)*, 2010 IEEE, pages 560–565. IEEE, 2010. 3
- [9] David T Hoffmann, Syed Haseeb Raza, Hanqiu Jiang, Denis Tananaev, Steffen Klingenhoefer, and Martin Meinke. Floxels: Fast unsupervised voxel based scene flow estimation. In Proceedings of the Computer Vision and Pattern Recognition Conference, pages 22328–22337, 2025. 3
- [10] Eddy Ilg, Nikolaus Mayer, Tonmoy Saikia, Margret Keuper, Alexey Dosovitskiy, and Thomas Brox. Flownet 2.0: Evolution of optical flow estimation with deep networks. In *Pro*ceedings of the IEEE conference on computer vision and pattern recognition, pages 2462–2470, 2017. 1
- [11] Philipp Jund, Chris Sweeney, Nichola Abdo, Zhifeng Chen, and Jonathon Shlens. Scalable scene flow from point clouds in the real world. *IEEE Robotics and Automation Letters*, 7 (2):1589–1596, 2021. 3
- [12] Ishan Khatri, Kyle Vedder, Neehar Peri, Deva Ramanan, and James Hays. I cant believe its not scene flow! In *European Conference on Computer Vision*, pages 242–257. Springer, 2024. 1, 3, 4, 5, 6, 11

- [13] Ajinkya Khoche, Qingwen Zhang, Laura Pereira Sanchez, Aron Asefaw, Sina Sharif Mansouri, and Patric Jensfelt. SSF: Sparse long-range scene flow for autonomous driving. In 2025 IEEE International Conference on Robotics and Automation (ICRA), pages 6394–6400, 2025. 3, 5
- [14] Jaeyeul Kim, Jungwan Woo, Jeonghoon Kim, and Sunghoon Im. Rethinking lidar domain generalization: Single source as multiple density domains. In *European Conference on Computer Vision*, pages 310–327. Springer, 2024. 1, 3
- [15] Jaeyeul Kim, Jungwan Woo, Ukcheol Shin, Jean Oh, and Sunghoon Im. Flow4D: Leveraging 4d voxel network for lidar scene flow estimation. *IEEE Robotics and Automation Letters*, pages 1–8, 2025. 1, 2, 3, 5
- [16] John Lambert, Zhuang Liu, Ozan Sener, James Hays, and Vladlen Koltun. Mseg: A composite dataset for multi-domain semantic segmentation. In *Proceedings of* the IEEE/CVF conference on computer vision and pattern recognition, pages 2879–2888, 2020. 1
- [17] Itai Lang, Dror Aiger, Forrester Cole, Shai Avidan, and Michael Rubinstein. Scoop: Self-supervised correspondence and optimization-based scene flow. In *Proceedings of* the IEEE/CVF Conference on Computer Vision and Pattern Recognition, pages 5281–5290, 2023. 3
- [18] Xueqian Li, Jhony Kaesemodel Pontes, and Simon Lucey. Neural scene flow prior. Advances in Neural Information Processing Systems, 34:7838–7851, 2021. 3, 5
- [19] Xueqian Li, Jianqiao Zheng, Francesco Ferroni, Jhony Kaesemodel Pontes, and Simon Lucey. Fast neural scene flow. In *Proceedings of the IEEE/CVF International Conference on Computer Vision*, pages 9878–9890, 2023. 3, 5
- [20] Yiqing Liang, Abhishek Badki, Hang Su, James Tompkin, and Orazio Gallo. Zero-shot monocular scene flow estimation in the wild. In *Proceedings of the Computer Vision and Pattern Recognition Conference*, 2025. 1
- [21] Yancong Lin and Holger Caesar. Icp-flow: Lidar scene flow estimation with icp. In CVPR, 2024. 5
- [22] Yancong Lin, Shiming Wang, Liangliang Nan, Julian Kooij, and Holger Caesar. Voteflow: Enforcing local rigidity in self-supervised scene flow. In *Proceedings of the Computer Vision and Pattern Recognition Conference*, pages 17155–17164, 2025. 5
- [23] Youquan Liu, Lingdong Kong, Xiaoyang Wu, Runnan Chen, Xin Li, Liang Pan, Ziwei Liu, and Yuexin Ma. Multi-space alignments towards universal lidar segmentation. In Proceedings of the IEEE/CVF Conference on Computer Vision and Pattern Recognition (CVPR), pages 14648–14661, 2024.
- [24] Jiehao Luo, Jintao Cheng, Xiaoyu Tang, Qingwen Zhang, Bohuan Xue, and Rui Fan. Mambaflow: A novel and flow-guided state space model for scene flow estimation. *arXiv* preprint arXiv:2502.16907, 2025. 3
- [25] Anish Madan, Neehar Peri, Shu Kong, and Deva Ramanan. Revisiting few-shot object detection with vision-language models. arXiv preprint arXiv:2312.14494, 2023. 3
- [26] Dušan Malić, Christian Fruhwirth-Reisinger, Samuel Schulter, and Horst Possegger. Gblobs: Explicit local structure via gaussian blobs for improved cross-domain lidar-based 3d

- object detection. In *Proceedings of the Computer Vision and Pattern Recognition Conference*, pages 27357–27367, 2025.
- [27] Björn Michele, Alexandre Boulch, Gilles Puy, Tuan-Hung Vu, Renaud Marlet, and Nicolas Courty. Saluda: Surfacebased automotive lidar unsupervised domain adaptation. In 2024 International Conference on 3D Vision (3DV), pages 421–431. IEEE, 2024. 3
- [28] Neehar Peri, Mengtian Li, Benjamin Wilson, Yu-Xiong Wang, James Hays, and Deva Ramanan. An empirical analysis of range for 3d object detection. In *Proceedings of the IEEE/CVF International Conference on Computer Vision*, pages 4074–4083, 2023. 2
- [29] Peter Robicheaux, Matvei Popov, Anish Madan, Isaac Robinson, Joseph Nelson, Deva Ramanan, and Neehar Peri. Roboflow100-vl: A multi-domain object detection benchmark for vision-language models. arXiv preprint arXiv:2505.20612, 2025. 3
- [30] Cristiano Saltori, Aljosa Osep, Elisa Ricci, and Laura Leal-Taixé. Walking your lidog: A journey through multiple domains for lidar semantic segmentation. In *Proceedings of* the IEEE/CVF international conference on computer vision, pages 196–206, 2023. 1
- [31] Louis Soum-Fontez, Jean-Emmanuel Deschaud, and François Goulette. Mdt3d: Multi-dataset training for lidar 3d object detection generalization. In 2023 IEEE/RSJ International Conference on Intelligent Robots and Systems (IROS), pages 5765–5772. IEEE, 2023. 1
- [32] Jiahao Sun, Chunmei Qing, Xiang Xu, Lingdong Kong, Youquan Liu, Li Li, Chenming Zhu, Jingwei Zhang, Zeqi Xiao, Runnan Chen, et al. An empirical study of training state-of-the-art lidar segmentation models. *arXiv preprint arXiv:2405.14870*, 2024. 3
- [33] Pei Sun, Henrik Kretzschmar, Xerxes Dotiwalla, Aurelien Chouard, Vijaysai Patnaik, Paul Tsui, James Guo, Yin Zhou, Yuning Chai, Benjamin Caine, et al. Scalability in perception for autonomous driving: Waymo open dataset. In *Proceedings of the IEEE/CVF conference on computer vision and pattern recognition*, pages 2446–2454, 2020. 1
- [34] Zachary Teed and Jia Deng. Raft: Recurrent all-pairs field transforms for optical flow. In *European conference on computer vision*, pages 402–419. Springer, 2020. 1
- [35] Kyle Vedder, Neehar Peri, Nathaniel Chodosh, Ishan Khatri, Eric Eaton, Dinesh Jayaraman, Yang Liu Deva Ramanan, and James Hays. ZeroFlow: Fast Zero Label Scene Flow via Distillation. *International Conference on Learning Representations (ICLR)*, 2024. 1, 3
- [36] Kyle Vedder, Neehar Peri, Ishan Khatri, Siyi Li, Eric Eaton, Mehmet Kemal Kocamaz, Yue Wang, Zhiding Yu, Deva Ramanan, and Joachim Pehserl. Neural eulerian scene flow fields. In *The Thirteenth International Conference on Learn*ing Representations, 2025. 1, 3, 5
- [37] Sundar Vedula, Peter Rander, Robert Collins, and Takeo Kanade. Three-dimensional scene flow. *IEEE transactions on pattern analysis and machine intelligence*, 27(3):475–480, 2005. 3
- [38] Chunwei Wang, Chao Ma, Ming Zhu, and Xiaokang Yang. Pointaugmenting: Cross-modal augmentation for 3d object

- detection. In *Proceedings of the IEEE/CVF conference* on computer vision and pattern recognition, pages 11794–11803, 2021. 3
- [39] Jingkang Wang, Henry Che, Yun Chen, Ze Yang, Lily Goli, Sivabalan Manivasagam, and Raquel Urtasun. Flux4d: Flow-based unsupervised 4d reconstruction. In *The Thirty-ninth Annual Conference on Neural Information Processing Systems*, 2025. 3
- [40] Ruicheng Wang, Sicheng Xu, Yue Dong, Yu Deng, Jianfeng Xiang, Zelong Lv, Guangzhong Sun, Xin Tong, and Jiaolong Yang. Moge-2: Accurate monocular geometry with metric scale and sharp details. *arXiv preprint arXiv:2507.02546*, 2025. 1
- [41] Yan Wang, Xiangyu Chen, Yurong You, Li Erran Li, Bharath Hariharan, Mark Campbell, Kilian Q Weinberger, and Wei-Lun Chao. Train in germany, test in the usa: Making 3d object detectors generalize. In *Proceedings of the IEEE/CVF conference on computer vision and pattern recognition*, pages 11713–11723, 2020. 1
- [42] Ziyi Wang, Yi Wei, Yongming Rao, Jie Zhou, and Jiwen Lu. 3d point-voxel correlation fields for scene flow estimation. IEEE Transactions on Pattern Analysis and Machine Intelligence, 2023. 3
- [43] Yi Wei, Ziyi Wang, Yongming Rao, Jiwen Lu, and Jie Zhou. PV-RAFT: Point-Voxel Correlation Fields for Scene Flow Estimation of Point Clouds. In CVPR, 2021. 3
- [44] Benjamin Wilson, William Qi, Tanmay Agarwal, John Lambert, Jagjeet Singh, and et al. Argoverse 2: Next generation datasets for self-driving perception and forecasting. In Proceedings of the Neural Information Processing Systems Track on Datasets and Benchmarks (NeurIPS Datasets and Benchmarks 2021), 2021.
- [45] Xiang Xu, Lingdong Kong, Hui Shuai, Wenwei Zhang, Liang Pan, Kai Chen, Ziwei Liu, and Qingshan Liu. Superflow++: Enhanced spatiotemporal consistency for crossmodal data pretraining. arXiv preprint arXiv:2503.19912, 2025. 3
- [46] Qingwen Zhang, Yi Yang, Heng Fang, Ruoyu Geng, and Patric Jensfelt. DeFlow: Decoder of scene flow network in autonomous driving. In 2024 IEEE International Conference on Robotics and Automation (ICRA), pages 2105–2111, 2024. 3, 5
- [47] Qingwen Zhang, Yi Yang, Peizheng Li, Olov Andersson, and Patric Jensfelt. SeFlow: A self-supervised scene flow method in autonomous driving. In European Conference on Computer Vision (ECCV), page 353369. Springer, 2024. 5
- [48] Qingwen Zhang, Ajinkya Khoche, Yi Yang, Li Ling, Sharif Mansouri Sina, Olov Andersson, and Patric Jensfelt. HiMo: High-speed objects motion compensation in point cloud. arXiv preprint arXiv:2503.00803, 2025. 5
- [49] Qingwen Zhang, Xiaomeng Zhu, Yushan Zhang, Yixi Cai, Olov Andersson, and Patric Jensfelt. DeltaFlow: An efficient multi-frame scene flow estimation method. *arXiv preprint* arXiv:2508.17054, 2025. 1, 3, 5
- [50] Yushan Zhang, Johan Edstedt, Bastian Wandt, Per-Erik Forssén, Maria Magnusson, and Michael Felsberg. Gmsf: Global matching scene flow. Advances in Neural Information Processing Systems, 36, 2024. 3

# A. Implementation Details

**Models.** We train and evaluate SSF and  $\Delta$ Flow using their official implementations without modification. As shown in Table 9, Flow4D benefits from a larger backbone when trained on the unified dataset. We denote this model as Flow4D-XL, which preserves the published architecture and increases all channel widths in the 4D Voxel Network by a uniform factor of three, with the Voxel Feature Encoders and Point Head adjusted accordingly to match the widened input/output dimensions. The full configuration is shown in Table 12. All dataset-specific Flow4D models use the original backbone, while all Flow4D models trained on the unified dataset use Flow4D-XL unless otherwise noted.

Table 12. Flow4D-XL 4D Voxel Network Architecture.

Stage	STDB-P (Filters)	Pool & Up (Kernel, Stride)	Output shape $[W \times L \times H \times T \times ch]$
Input	-	-	$512 \times 512 \times 32 \times 5 \times 48$
1	(48, 96) (96, 96)	Pool (2,2,2,1)	$256\times256\times16\times5\times96$
2	(96, 192) (192, 192)	Pool (2,2,2,1)	$128\times128\times8\times5\times192$
3	(192, 192) (192, 192)	Pool (2,2,2,1)	$64 \times 64 \times 4 \times 5 \times 192$
4	(192, 192) (192, 192)	Pool (2,2,1,1)	$32 \times 32 \times 4 \times 5 \times 192$
5	(192, 192) (192, 192)	Up (2,2,1,1)	$32\times32\times4\times5\times192$
6	(192, 192) (192, 192)	Up (2,2,2,1)	$64\times64\times4\times5\times192$
7	(192, 192) (192, 192)	Up (2,2,2,1)	$128\times128\times8\times5\times192$
8	(192, 192) (192, 192)	Up (2,2,2,1)	$256\times256\times16\times5\times192$
9	(96, 48)	_	$512 \times 512 \times 32 \times 5 \times 48$

**Augmentations.** We apply two dataset-agnostic augmentations. Following  $\Delta Flow$ , we apply height jitter with probability 0.8 by translating the point cloud along the sensors z-axis using a uniform offset in the range of [0.5, 2.0] m. To improve cross-dataset density generalization, we also apply LiDAR beam dropout with probability 0.35, removing every other LiDAR beam for all Waymo and Argoverse 2 sweeps so that the effective density approximates a 32-beam sensor.

Training Settings. For the Argoverse 2 benchmark, we follow the standard evaluation protocol and report test-set performance according to the official public leaderboard to ensure fair comparison. For all TruckScenes experiments, baseline methods and their UniFlowvariants are trained under the same setups described in their respective original papers. UniFlow models adopt identical architectures unless otherwise noted, and all models are trained until convergence. We apply height augmentation to UniFlow and all dataset-specific  $\Delta$ Flow models to match the original training setup, and apply sparsity augmentation only to UniFlow models.

## B. Ablation on Synthetic Sparse LiDARs

We evaluate the performance of UniFlow models on synthetically sparsified LiDAR point clouds to investigate the

impact of LiDAR sparsity on cross-domain generalization. We do not train any new models; all results are from models trained on the original datasets. Sparse datasets are created by removing every other beam from each LiDAR sweep. As shown in Table 13, the colored deltas indicate the change in performance relative to each models performance on the standard datasets (higher EPE indicates worse performance). Across datasets, degradation correlates strongly with dataset sparsity: models evaluated on Sparse nuScenes perform the worst due to its low (16-beam) density, while models evaluated on Sparse Waymo are affected the least due to its substantially higher point density.

Notably, UniFlow models are consistently more robust than dataset-specific baselines, exhibiting smaller performance drops across all datasets. This suggests that multidataset training provides useful regularization even under extreme sparsity.

### C. Ablation on Velocity Augmentation

Our velocity-bucket analysis in Figure 2 suggests that the velocity domain gap between training datasets is highly correlated with cross-domain generalization. To test whether increasing the proportion of fast motion improves flow estimation on fast moving objects across datasets, we create a fast version of each dataset by down-sampling each dataset from 10Hz to 5Hz and add these sequences to the unified training set. This effectively doubles the speed of all dynamic objects and shifts the velocity distribution to the right (Figure 5). As shown in Table 14, this improves performance in the highest-speed bucket  $(2.0, \infty)$ , but consistently degrades accuracy for all other velocity buckets. We attribute this to the aggressiveness of the augmentation: doubling the speed of every dynamic object produces unrealistic trajectories that no longer resemble any real object motion. Although the velocity domain gap significantly contributes to cross-domain generalization, naively downsampling datasets to increase the proportion of fast moving objects does not improve performance. Future work should consider different strategies for effective velocity augmentation.

#### D. Performance Breakdown on TruckScenes

We present a detailed breakdown between three-way EPE and dynamic bucket-normalized EPE performance on TruckScenes to investigate the inconsistent trends found in the main paper. As demonstrated by Khatri et. al. [12], three-way EPE directly measures absolute endpoint error and therefore scales with the magnitude of the ground-truth flow. As a result, underestimating large displacement vectors from fast moving objects in highway scenes incurs disproportionately high penalties, inflating three-way EPE for TruckScenes. In contrast, dynamic bucket-normalized

Table 13. **Ablation on Synthetic Sparse LiDARs.** We evaluate methods on synthetically sparsified LiDAR sweeps, created by removing every other beam from the original sensors. Colored numbers indicate the change relative to the original dense setting, with red showing degradation and blue showing improvement. Lower is better.

M-41- J		Three-way l	EPE (cm) ↓		Dynamic Bucket-Normalized ↓						
Method	Mean	FD	FS	BS	Dynamic M	CAR	OTHER	PED	VRU		
Sparse AV2											
SSF	4.51 <sub>↑0.44</sub>	10.79 <sub>↑1.10</sub>	1.96 <sub>↑0.21</sub>	0.80 <sub>10.01</sub>	0.289 10.041	0.183 0.016	0.329 \(\frac{1}{10.061}\)	0.336 0.054	0.309 \(\frac{1}{10.032}\)		
SSF (UniFlow, Ours)	3.73 ↑0.24	$9.29_{\ 10.62}$	1.38 ↑0.11	0.53 \(\frac{1}{10.01}\)	0.240 10.018	0.160 0.009	0.168 10.003	0.328 \(\frac{1}{10.040}\)	$0.304_{0.019}$		
Flow4D	3.99 ↑0.37	9.58 <sub>↑1.03</sub>	1.70 <sub>↑0.08</sub>	0.69 <sub>↑0.00</sub>	0.209 10.017	0.158 <sub>\(\frac{1}{10.012}\)</sub>	0.183 0.019	$0.238_{\ \ \ \ \ \ \ \ \ \ \ \ \ \ \ \ \ \ \ $	$0.255_{\ \uparrow 0.020}$		
Flow4D (UniFlow, Ours)	3.44 ↑0.20	8.27 <sub>10.99</sub>	1.39 <sub>↑0.13</sub>	0.65 <sub>↑0.02</sub>	0.181 10.005	0.138 10.005	$0.151_{\ \uparrow 0.002}$	$0.198_{\ \downarrow 0.005}$	$0.237_{\ \uparrow 0.017}$		
$\Delta$ Flow	3.30 ↑0.26	8.00 <sub>10.67</sub>	1.22 <sub>↑0.09</sub>	0.67 <sub>↑0.03</sub>	0.218 10.042	0.149 <sub>\(\frac{1}{10.013}\)</sub>	0.169 \(\frac{1}{10.008}\)	$0.230_{\ \ \ \ \ \ \ \ \ \ \ \ \ \ \ \ \ \ \ $	$0.218_{\  au0.005}$		
$\Delta$ Flow (UniFlow, Ours)	3.19 <sub>↑0.17</sub>	7.53 <sub>↑0.40</sub>	1.25 <sub>↑0.07</sub>	0.77 <sub>↑0.03</sub>	0.182 ↑0.010	$0.141_{\ \uparrow 0.008}$	$0.157_{\ \uparrow 0.002}$	$0.219_{\ \uparrow 0.025}$	$0.213_{\   \uparrow 0.004}$		
Sparse Waymo											
SSF	2.45 10.24	6.12 <sub>↑0.50</sub>	0.92 <sub>↑0.18</sub>	0.30 <sub>↑0.05</sub>	0.217 \$\psi_{0.040}\$	0.100 <sub>↑0.003</sub>	-	$0.342_{\downarrow 0.127}$	0.210 \(\frac{1}{10.003}\)		
SSF (UniFlow, Ours)	2.02 10.17	5.22 <sub>↑0.36</sub>	0.65 \(\tau_{0.10}\)	0.18 \(\dagger_{0.05}\)	0.199 \$\tau_{0.042}\$	0.085 10.004	-	$0.318_{\pm 0.139}$	0.193 <sub>10.010</sub>		
Flow4D	2.00 ↑0.18	4.92 <sub>↑0.34</sub>	0.76 <sub>↑0.15</sub>	0.33 ↑0.05	0.196 10.018	0.076 10.001	-	$0.363_{\ \downarrow 0.059}$	0.150 \(\dagger_{0.004}\)		
Flow4D (UniFlow, Ours)	1.66 ↑0.05	3.92 ↑0.09	0.73 <sub>10.05</sub>	$0.31_{\downarrow 0.02}$	0.143 10.046	$0.063_{\downarrow 0.001}$	-	$0.249_{\ \downarrow 0.151}$	$0.119_{\ 10.015}$		
$\Delta$ Flow	1.53 ↑0.09	3.42 <sub>↑0.12</sub>	0.68 \(\tau_{0.08}\)	0.50 <sub>10.09</sub>	0.146 \$\psi_{0.050}\$	$0.072_{\   \uparrow 0.002}$	-	$0.257_{\downarrow 0.154}$	0.107 <sub>↑0.000</sub>		
$\Delta$ Flow (UniFlow, Ours)	1.43 <sub>↑0.05</sub>	3.12 <sub>↑0.05</sub>	0.66 \(\phi_{0.05}\)	0.52 \(\phi_{0.06}\)	0.138 \$\psi_{0.050}\$	0.066 <sub>↑0.001</sub>	-	$0.246_{\ \downarrow 0.157}$	0.102 <sub>↑0.006</sub>		
Sparse nuScenes											
SSF	3.96 ↑0.96	9.24 <sub>12.69</sub>	2.18 <sub>↑0.14</sub>	0.45	0.298 +0.078	0.173 <sub>10.031</sub>	0.223 10.027	0.556 0.158	0.241 \(\frac{1}{10.096}\)		
SSF (UniFlow, Ours)	2.94 ↑1.05	7.11 <sub>↑3.01</sub>	1.56 ↑0.13	0.14 <sub>↑0.01</sub>	0.222 10.089	$0.094_{\ \ \ \ \ \ \ \ \ \ \ \ \ \ \ \ \ \ \ $	0.165 \(\tau_{0.034}\)	$0.454_{0.225}$	0.173 <sub>↑0.083</sub>		
Flow4D	4.31 ↑0.86	10.41 <sub>↑2.44</sub>	1.92 <sub>↑0.07</sub>	0.61 <sub>↑0.06</sub>	0.309 ↑0.078	$0.227_{0.067}$	0.283 10.042	$0.439_{\ \ \ \ \ \ \ \ \ \ \ \ \ \ \ \ \ \ \ $	0.287 <sub>10.056</sub>		
Flow4D (UniFlow, Ours)	3.72 <sub>↑0.71</sub>	9.31 <sub>12.03</sub>	$1.52_{\ \uparrow 0.05}$	0.31 <sub>↑0.03</sub>	0.279 ↑0.083	0.140 <sub>\(\tau_0.003\)</sub>	0.266	0.430 10.158	$0.279_{\   \uparrow 0.122}$		
$\Delta$ Flow	2.76 10.71	6.06 <sub>1.87</sub>	1.46 <sub>10.10</sub>	0.75 <sub>↑0.16</sub>	0.255 10.081	$0.179_{\   \uparrow 0.047}$	0.217 10.033	0.409 10.148	$0.214_{\ \ \ \ \ \ \ \ \ \ \ \ \ \ \ \ \ \ \ $		
$\Delta$ Flow (UniFlow, Ours)	2.25 †0.62	4.81 <sub>↑1.63</sub>	1.43 <sub>↑0.14</sub>	0.51 \(\phi_{0.09}\)	0.206 ↑0.067	0.126 <sub>↑0.028</sub>	0.170 <sub>↑0.033</sub>	0.365 ↑0.133	$0.165_{\ \uparrow 0.074}$		

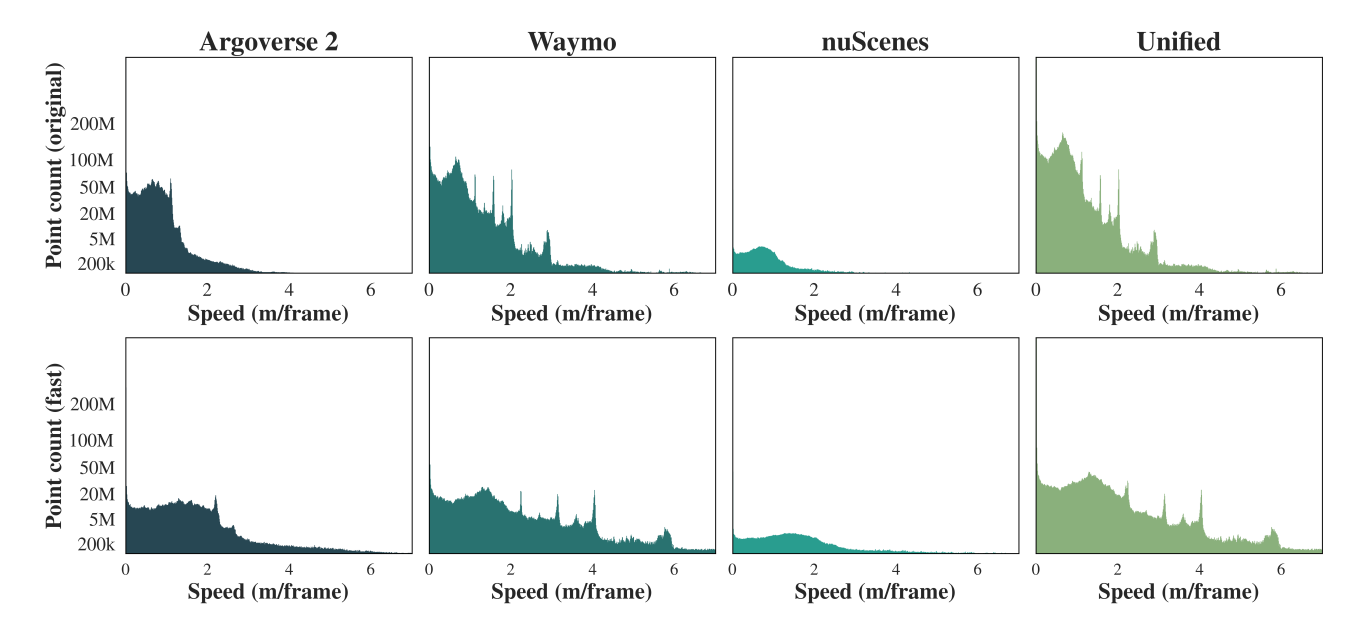


Figure 5. Comparing Original and Downsampled Velocity Distributions. We plot the velocity distributions of the original AV2, Waymo, and nuScenes training sets (top row), their corresponding down-sampled "fast" versions (bottom row), and the unified distribution that combine the three datasets (right column).

EPE offers a more balanced assessment of model predictions by evaluating error relative to object speed. As shown in Table 15, UniFlow achieves strong zero-shot generalization compared to in-domain models across commonspeed buckets (0 to 2.0 m/frame), indicating that Uni-

Flow effectively models the motion patterns dominating most scenes. We find that UniFlow models perform worse than in-domain models in the high-speed regime (>2.0 m/frame), suggesting that future work should explicitly address high-speed scene flow.

Table 14. **Velocity Augmentation.** We perform velocity augmentation by adding fast versions of each dataset to the unified dataset, and compare the results to Flow4D and Flow4D (UniFlow) trained on the original 10 Hz data. We denote zero-shot evaluation with <sup>ZS</sup> for cases where the model has never seen the target domain during training.

Modbad	Dyı	namic Bu	cket-Norma	Speed Bucket-Normalized ↓					
Method	Dynamic M	CAR	OTHER	PED	VRU	[0,0.5]	(0.5,1.0]	(1.0,2.0]	(2.0,∞]
Argoverse 2									
Flow4D	0.192	0.146	0.164	0.221	0.236	0.020	0.119	0.114	0.103
Flow4D (UniFlow, Ours)	0.176	0.133	0.149	0.203	0.220	0.018	0.107	0.108	0.091
Flow4D (Fast-UniFlow, Ours)	0.179	0.134	0.154	0.204	0.224	0.019	0.114	0.111	0.085
Waymo									
Flow4D	0.214	0.074	-	0.423	0.146	0.007	0.064	0.051	0.130
Flow4D (UniFlow, Ours)	0.191	0.064	-	0.400	0.110	0.006	0.053	0.042	0.128
Flow4D (Fast-UniFlow, Ours)	0.208	0.066	-	0.409	0.149	0.007	0.058	0.043	0.093
nuScenes									
Flow4D	0.230	0.160	0.241	0.345	0.176	0.013	0.100	0.109	0.370
Flow4D (UniFlow, Ours)	0.196	0.137	0.219	0.272	0.157	0.009	0.082	0.089	0.374
Flow4D (Fast-UniFlow, Ours)	0.187	0.126	0.217	0.263	0.143	0.009	0.090	0.101	0.306
TruckScenes									
Flow4D	0.456	0.176	0.351	0.885	0.413	0.054	0.192	0.171	0.091
Flow4D (UniFlow, Ours) ZS	0.281	0.088	0.277	0.530	0.230	0.034	0.097	0.119	0.389
Flow4D (Fast-UniFlow, Ours) <sup>ZS</sup>	0.281	0.079	0.264	0.546	0.235	0.034	0.112	0.106	0.323

Table 15. **Performance Breakdown on TruckScenes.** Three-way EPE heavily penalizes fast-moving objects and is biased towards fast-moving highway scenes. In contrast, Dynamic Bucket-Normalized EPE provides a more fair comparison across object categories and speeds.

Method	Three-way EPE (cm) ↓				Dynamic Bucket-Norm. ↓				Speed Bucket-Norm. ↓				
	Mean	FD	FS	BS	Dyn. M	CAR	OTHER	PED	VRU	[0,0.5]	(0.5,1.0]	(1.0,2.0]	$(2.0,\infty]$
SSF	6.20	15.17	1.01	2.44	0.453	0.215	0.308	0.875	0.414	0.055	0.190	0.173	0.086
SSF (UniFlow, Ours)	35.23	103.72	1.69	0.27	0.435	0.149	0.455	0.669	0.466	0.036	0.148	0.285	0.637
Flow4D	16.14	44.87	1.71	1.85	0.456	0.176	0.351	0.885	0.413	0.027	0.249	0.157	0.079
Flow4D (UniFlow, Ours)	23.59	68.41	1.78	0.57	0.281	0.088	0.277	0.530	0.230	0.034	0.097	0.119	0.389
$\Delta$ Flow	7.28	16.26	1.36	4.52	0.402	0.196	0.400	0.690	0.323	0.079	0.222	0.203	0.102
$\Delta$ Flow (UniFlow, Ours)	15.76	45.76	1.02	1.32	0.283	0.101	0.293	0.513	0.226	0.039	0.094	0.127	0.429

# E. Visualizing Failure Cases

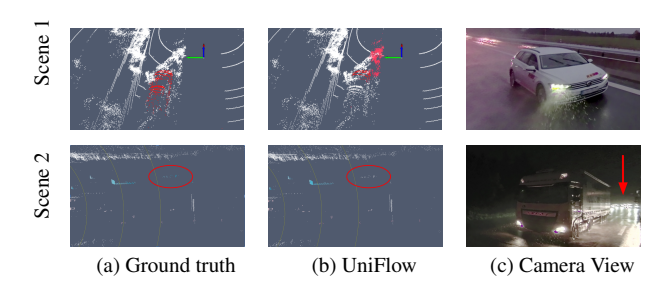


Figure 6. **Failure Case Visualizations.** We show two failure cases of Flow4D (UniFlow). Each example includes the ground-truth flow (left), the model prediction (middle), and the corresponding RGB frame (right).

Figure 6 illustrates two representative failure modes of UniFlow models. In the first example, adverse weather introduces dense rain streaks that create spurious LiDAR returns, leading the model to produce localized artifacts. In

the second example, extreme sparsity at long range causes the model not estimate flow for an object located nearly 100m away.

#### F. Supplementary Video

We include a supplementary video on our project page, where we visualize scene flow predictions on a challenging rainy sequence from TruckScenes. As shown in the video,  $\Delta Flow$  frequently produces artifacts on rain streaks and background points, which become especially pronounced during occlusions.  $\Delta Flow$  also predicts inconsistent flow vectors on dynamic objects. In contrast,  $\Delta Flow$  (UniFlow) yields significantly more stable and coherent motion fields.